

Computational and Experimental Studies on HEF 7100 Two-phase Spray Cooling

Ali Sadaghiani¹, Behnam Parizad Benama¹, Osman Akdağ², Samet Saygan^{2,§}, Ali Koşar¹

¹ Sabanci University, Orhanli, 34956, Tuzla, Istanbul, Turkey

a.sadaghiani@sabanciuniv.edu; bparizadbenam@sabanciuniv.edu, kosara@sabanciuniv.edu

² ASELSAN Inc., 06200, Yenimahalle, Ankara, Turkey (§ Former employee)

oakdag@aselsan.com.tr, sametsaygan@gmail.com

Abstract - Spray cooling is a highly efficient thermal management technique that has gained significant attention in various industrial and technological applications, such as power electronics, high-power lasers, and conversion systems. This investigation examines the effects of HEF 7100 spray parameters on the cooling process using numerical models and experimental approaches. We performed a series of tests to carefully examine the spray characteristics by progressively increasing the heat flux applied to a 2 cm² hotspot. A comprehensive analysis of the effect of spray parameters was performed using two-phase curves, which depict the relationship between surface temperature and heat flux during the cooling process. Numerical simulations were performed to understand the fundamental principles underpinning heat transfer during multiple droplet impacts. It was found that the spray angle plays a substantial role in heat transfer, reducing heat transfer rates as the angle widens. This effect diminishes with increased spray pressure and temperature due to reduced surface wetting area and liquid film thickening. Interestingly, nozzle temperature has minimal influence on pressure-induced surface temperature reduction. Moreover, nozzle pressure enhances spray performance, with higher enhancement observed in single-phase regions ($T_{\text{wall}} < T_{\text{sat}}$). This influence strengthens with decreasing spray angles and shorter spray distances in flat nozzles. The obtained boiling curves and heat transfer coefficients provide valuable data for designing and optimizing spray cooling systems, ultimately promoting the efficient dissipation of high heat fluxes in various engineering applications.

Keywords: Spray Cooling, Thermal management, HEF 7100 dielectric coolant, Two-phase numerical model, Experimental study, Parametric study

1. Introduction

Efficient cooling techniques are paramount in current thermal management and energy systems due to escalating heat generation in these systems, especially in the context of escalating heat generation from devices and processes [1-3]. This is crucial in preventing device failure, enhancing performance, and extending operational lifespans in various industrial applications, such as electronic devices, aerospace applications, and energy generation sectors [4, 5]. In electronic devices like computer chips and power electronics, effective cooling is essential to dissipate the high heat fluxes generated by these components, which is vital to prevent overheating and ensure optimal performance.

Traditional cooling methods are increasingly inadequate in meeting these evolving demands. This has led to a surge in the exploration of new cooling technologies characterized by large cooling capacities, fast cooling rates, and temperature uniformity. Spray cooling, involving the atomization of a liquid into a fine spray directed onto a heated surface, has emerged as a versatile and effective technique in this regard [6]. The efficacy of spray cooling is attributed to the large surface area of the droplets and the latent heat of vaporization, which facilitates efficient heat transfer. This method has been shown to offer significantly higher heat transfer coefficients compared to traditional methods like air/liquid natural and forced convection [7-9].

Several parameters, such as spray distance, pressure, angle, and temperature, influence spray cooling system performance. The spray distance, referring to the gap between the nozzle and the target surface, affects the droplet size and impact characteristics [10]. The spray pressure plays a crucial role in determining the velocity and momentum of the droplets, impacting the heat transfer rate [11]. The spray angle influences the coverage area and distribution of the spray on the surface [12], while the spray temperature affects the cooling capacity and the temperature gradient across the surface [13]. Studies like those of Tsutsumi et al. [14] and Tian et al. [15] have extensively investigated these parameters. For example, Tsutsumi

et al. [24] explored how varying the nozzle distance during spray quenching of aluminum alloy 2024 impacts the critical heat flux (CHF) and surface temperature, finding a complex relationship where CHF first decreases to a minimum value with increasing nozzle distance before decreasing upon further increase. Tian et al. [15] used numerical simulations to analyze the effect of spray pressure on cooling effectiveness in cryogenic applications, observing that higher spray pressures enhanced the heat transfer rate and cooling efficiency.

In addition to these factors, the characteristics of droplet impact are critical. Bao et al. [16] and Ruan et al. [17] investigated the influence of droplet diameter and velocity on cooling. Their findings underscored that larger droplet diameters and higher impact velocities significantly increase the maximum cooling factor. Ruan et al. [17] noted a linear increase in droplet evaporation with decreasing droplet diameter.

Numerical analysis is a pivotal tool in this realm, offering profound insights into the complex interaction of fluid dynamics, heat transfer, and phase change phenomena associated with droplet impact. Techniques such as the Volume of Fluid (VOF) and Coupled Level Set and Volume of Fluid (CLSVOF) methods have been pivotal in these studies [18-22]. For instance, Tao et al. [23] investigated the effect of droplet spacing on film dynamics in multiple droplet impacts, finding that droplet spacing significantly influences the spreading diameter and jet angle. Cao et al. [24] explored the impact angle and reported that varying the tangential velocity and liquid film thickness has opposite effects on crown evolution, highlighting the complex interplay of factors in spray cooling.

The heat transfer characteristics during droplet impact on liquid films have also been a major focus. Trujillo and colleagues [25] characterized the impact zone in periodic droplet impact, while Liang et al. [26] investigated droplet impact on a flowing liquid film. Li and Duan [27] focused on air entrapment during diesel droplet impact on inclined wet surfaces, emphasizing how trapped air significantly affects heat transfer at the early stages of impact. This highlights the multifaceted nature of spray cooling, where variables like impact velocity, liquid properties, and droplet spacing intertwine to define the cooling efficiency.

Despite extensive research, there remains a gap in understanding the synergistic effect of different impact parameters on heat transfer performance during the phase change process. This study aims to address these gaps by combining experimental and numerical analyses, using advanced techniques and simulations to elucidate the relationships between various parameters and their effects on heat transfer and cooling efficiency. Our work contributes to optimizing thermal management systems, providing valuable guidelines for designing efficient cooling strategies for diverse applications.

2. Materials and Methods

2.1. Test section and experimental setup

Fig. 1 illustrates the configuration of the experimental setup and test section. The core feature is a 2 cm² hot spot heated through cartridge heaters placed inside an aluminum block, with a Teflon layer for thermal insulation. The test section's side walls are constructed from polycarbonate glass and feature two distinct outlets on each side for liquid and vapor. Five spray nozzle housings were integrated into the test section to study the effects of spray-to-surface distance and angle. These housings accommodate Flat Fan UniJet® Nozzles (from Spraying System Co.) that generate 200-300µm droplets at a 120° cone angle.

HEF 7100 was used as the working fluid, with its thermophysical properties detailed in Table 1. The coolant is circulated from a reservoir in the setup, passing through a 2µm filter (Swagelok) to ensure purity. A preheater regulates the temperature of the fluid before it reaches the spray nozzles. Key measurements, such as the pressure and temperature of the fluid, are taken at the test section's inlet. The two-phase flow exiting the test section is then directed to a condenser. Here, both the inlet's two-phase flow and the outlet's liquid flow undergo temperature and pressure measurements via thermocouples and pressure transducers. The setup forms a closed loop, with the condenser outlet returning fluid to the reservoir. The pump in the system is adjustable, enabling different mass fluxes ranging from 100 to 500 ml/min, and can operate under pressures varying from 1 to 5 bars.

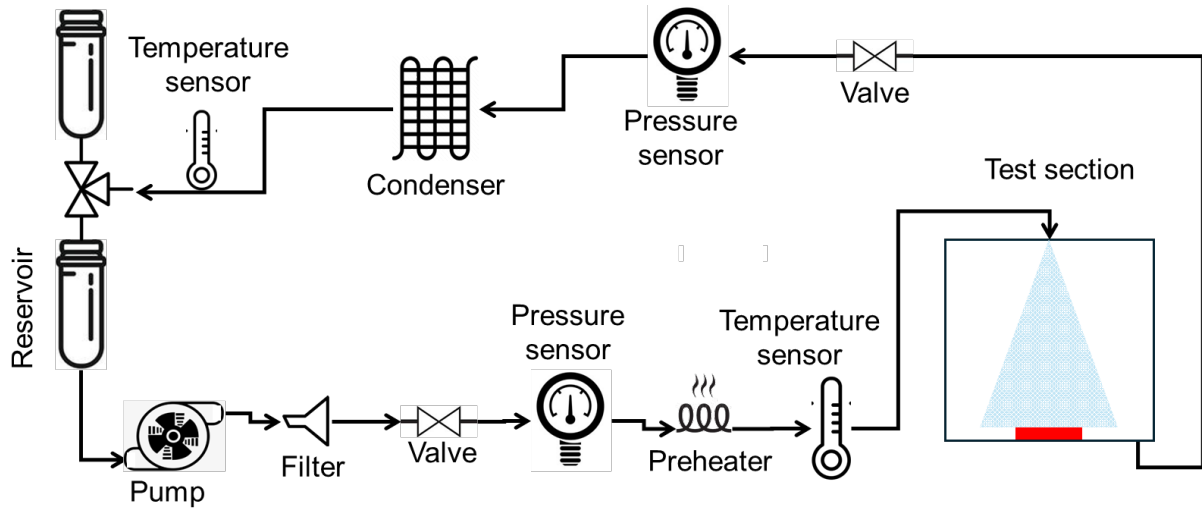


Fig. 1: Diagram of the closed loop HEF 7100 spray cooling setup

Table 1: Thermophysical properties of the working fluid.

Thermophysical properties	Working fluid (HEF7100)
Boiling point	61 (°C)
Molecular Weight	250 (g/mol)
Liquid Density	1510 (kg/m ³)
Surface Tension	13.6 (mN/m)
Latent Heat of Vaporization	112 (kJ/kg)
Specific Heat	1183 (J/kg.K)
Thermal Conductivity	0.069 (W/mK)

2.2. Computational domain

Fig. 2 depicts the computational domain used in the study, comprising two primary regions: the liquid domain, which includes a liquid film of thickness 'Th' and an impacting droplet with diameter 'D', and the vapor domain. The bottom wall is subjected to a contact heat flux, while the top surface is assigned an outlet boundary condition. The droplet impact analysis uses the Level Set (LS) method [28] (Eq. 1). The LS function, ϕ_{LS} , represents the interface between liquid ($\phi_{LS} < 0.5$) and air ($\phi_{LS} > 0.5$) and is advanced using a flow field to address moving boundary challenges. Interface equations are integrated with incompressible Navier–Stokes and continuity equations, considering factors like pressure, density, viscosity, and surface tension. The Lee model [29] is used for mass transfer simulation. The interfacial force is calculated using surface tension and interface curvature. The k- ϵ realizable turbulence model is used where liquid and vapor domains are incompressible. The study assumes a static contact angle of 90 degrees for simplicity, although the model can analyze various angles. Eqs. (1) to (8) below represent the transport equations.

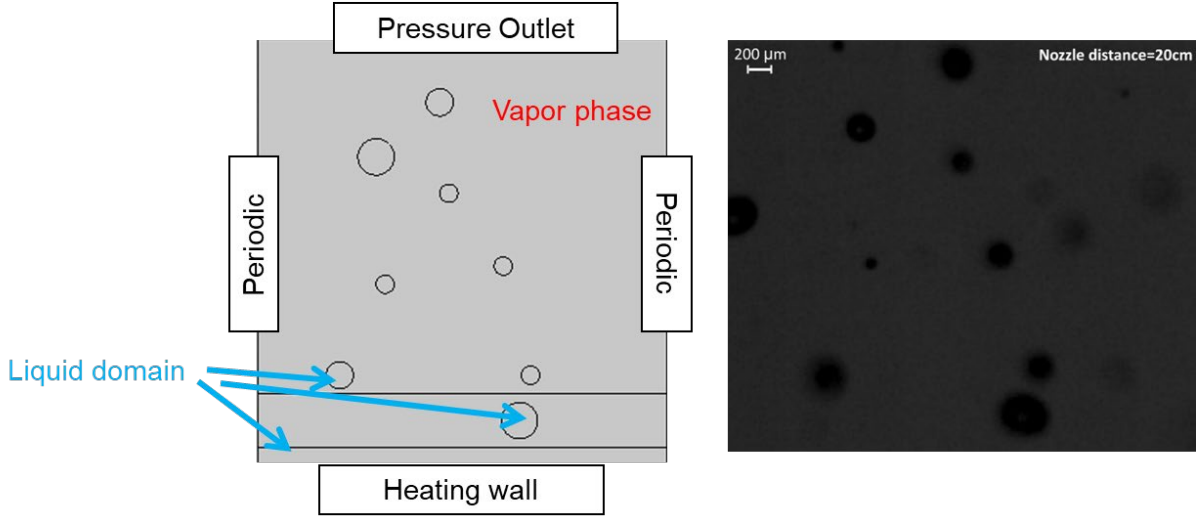


Fig. 2: Schematic of the numerical domain (left) based on experimental image (right)

$$\text{LS Equation} \quad \frac{\partial \phi_{LS}}{\partial t} + u \cdot \nabla \phi_{LS} = \omega \nabla \cdot (\epsilon_{ls} \nabla \phi_{LS} - \phi_{LS} (1 - \phi_{LS}) n) \quad (1)$$

$$\text{Mass Conservation} \quad \nabla \cdot (u) = S_1 \quad (2)$$

$$\text{Momentum Conservation} \quad \rho \phi \frac{\partial u}{\partial t} + \rho \phi_{LS} u \cdot \nabla u = -\nabla p + \nabla \cdot \left[\mu (\phi_{LS}) (\nabla u + (\nabla u)^T) \right] + \rho \phi_{LS} g + F_{st} \quad (3)$$

$$\text{Energy Conservation} \quad \rho C_p \frac{\partial T}{\partial t} + \rho C_p u \cdot \nabla T = \nabla \cdot (k \nabla T) + S_2 \quad (4)$$

$$\text{Mass exchange terms} \quad S_1 = \dot{m}_g = -\dot{m}_f = r_i \alpha_f \rho_f \frac{(T - T_{sat})}{T_{sat}} \quad (5)$$

$$S_2 = q = \dot{m}_g h_{fg} \quad (6)$$

$$\rho (u \cdot \nabla) u = \nabla \cdot \left[\left(\mu + \frac{\mu_T}{\sigma_k} \right) \right] + p_k - \rho \epsilon \quad (7)$$

$$\text{Turbulence model} \quad \rho (u \cdot \nabla) u = \nabla \cdot \left[\left(\mu + \frac{\mu_T}{\sigma_\epsilon} \right) \nabla \epsilon \right] + C_1 \rho s \epsilon - \frac{\rho \epsilon^2}{k + \sqrt{v \epsilon}} \quad (8)$$

3. Results and discussion

The effect of the impact angle on the boiling curve at an inlet temperature of 23°C and nozzle-to-surface distance of 3cm is shown in Fig. 2a. A deterioration in the heat transfer rate is observed for flat sprays when the spray angle is decreased. The main reason could be the reduction of the surface wetted area with the spray angle, which reduces the heat transfer rate and increases surface temperature (Fig. 2b). Similar observations are reported in the literature for full cone spray. Fig. 2c shows the effect of spray inlet temperature at nozzle-to-surface distance of 3cm and spray impact angles of 30° and 90°. The slope of the heat flux-wall superheat diagram indicates the heat transfer rate; a lower slope suggests a lower heat transfer coefficient. In the single-phase region (negative wall superheat values), forced convection is the primary heat transfer mechanism. In contrast, in the two-phase region (positive superheats), the enhanced cooling

rate is attributed to the latent heat of vaporization. Therefore, a higher temperature difference between the heated surface and the coolant (subcooling temperature) at lower spray temperatures leads to increased heat transfer rates and reduced surface temperatures in the single-phase region. In the two-phase region, both spray temperatures exhibit similar slopes, indicating that the latent heat component of heat transfer is predominant, regardless of the inlet temperature. The effect of spray temperature is more pronounced at a spray angle of 30°.

Fig.2d illustrates the distance effect on boiling curve at two inlet temperatures. At room inlet temperature, the spray is divided into single-phase and two-phase regions, differentiated by surface temperatures below or above the saturation temperature ($T_{sat} = 61^\circ\text{C}$). It's clear that the distance between the nozzle and the surface positively impacts the heat transfer rate. This impact is especially noticeable at the saturation inlet temperature. As indicated in Fig. 2b, the area covered by the flat spray expands as the distance from the nozzle outlet increases. This effective area enlargement enhances its cooling capacity by covering more of the hot spot zone.

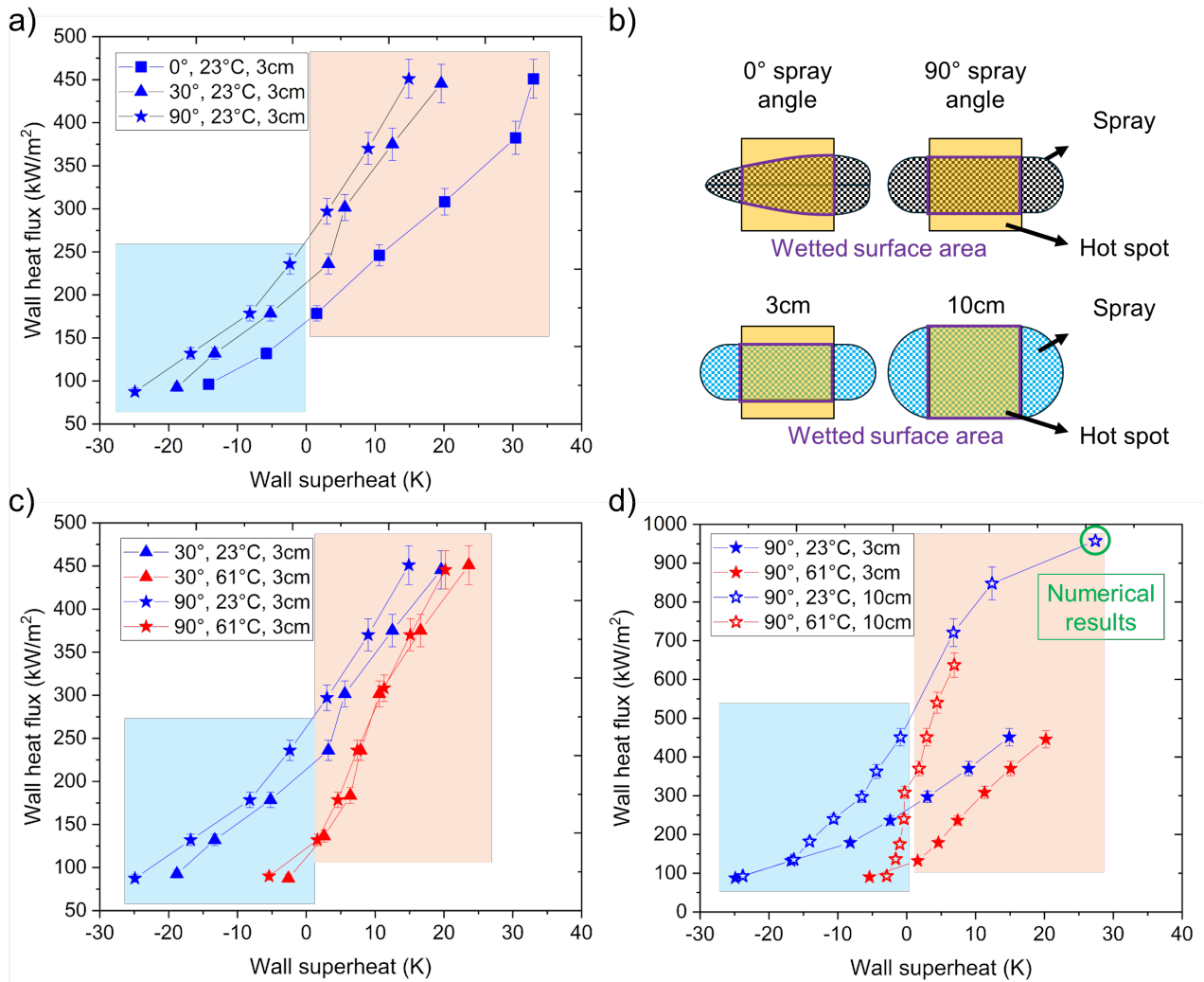


Fig. 3: a) effect of spray angle on wall superheat-heat flux diagram, b) schematic of the effect of spray angle and nozzle distance on spray coverage, c) effect of inlet temperature on boiling curve, d) effect of nozzle-to-surface distance on heat flux-wall superheat diagrams.

The developed model was used to simulate the spray cooling on a surface with a wall heat flux of 100 W/cm^2 and an initial liquid film thickness of $200 \mu\text{m}$. As stated, the computational domain replicates the experimental results of multiple droplet impact on a liquid film. Fig.4 shows the local surface heat flux and temperature for 10ms. According to the experimental results, on average, one droplet (in the form of successive droplets) impacts the surface every 3ms. As shown in Fig. 4, with an applied wall heat flux of 100 W/cm^2 , the spray cooling method keeps the surface temperature $\sim 90^\circ\text{C}$ ($\Delta T_{\text{superheat}}=29 \text{ K}$) throughout this 3ms period.

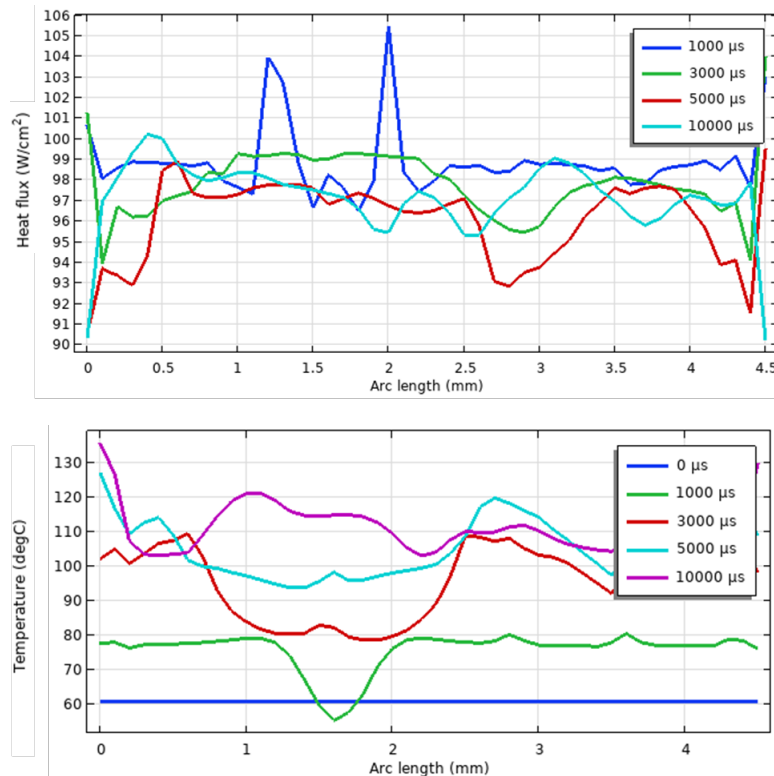


Fig. 4: a) effect of spray angle on wall superheat-heat flux diagram, b) numerical results obtained for liquid film and wall temperature variation with impact angle

4. Conclusion

Spray cooling is critical for heat management in high-heat flux electronic systems. Despite extensive research in spray cooling, flat sprays have been left unexamined. They are especially beneficial in tight spaces due to their uniform, wide coolant spread. This study uses numerical and experimental methods to examine key parameters of flat spray—spray angle, distance, and inlet temperature. The major findings are as follows:

1. Increased nozzle-to-surface distance improves heat transfer in flat sprays, unlike full cone sprays.
2. The heat transfer rate decreases with spray angle, and its impact diminishes with spray temperature.
3. Higher spray inlet temperatures result in increased wall superheats.
4. The developed numerical model demonstrates strong agreement with experimental results, indicating its reliability and effectiveness as a robust tool for spray cooling applications.

While this research underscores flat sprays' efficiency at lower flow rates compared to full cone sprays, future work should assess their long-term reliability, maintenance needs, and effectiveness in various environments and applications.

Acknowledgments

This study was supported by the internal fund of the Communication and Information Technologies Division of ASELSAN Inc. for Academic Collaborative Projects, Project number E.A.CF-22-02526.

References

1. Visaria, M. and I. Mudawar, *Application of Two-Phase Spray Cooling for Thermal Management of Electronic Devices*. IEEE Transactions on Components and Packaging Technologies, 2009. **32**(4): p. 784-793.
2. Parizad Benam, B., A.K. Sadaghiani, V. Yağcı, M. Parlak, K. Sefiane, and A. Koşar, *Review on high heat flux flow boiling of refrigerants and water for electronics cooling*. International Journal of Heat and Mass Transfer, 2021. **180**: p. 121787.
3. Kandasamy, R., J.Y. Ho, P. Liu, T.N. Wong, K.C. Toh, and S. Chua, Jr., *Two-phase spray cooling for high ambient temperature data centers: Evaluation of system performance*. Applied Energy, 2022. **305**: p. 117816.
4. Xiao, M., L. Tang, X. Zhang, I.Y.F. Lun, and Y. Yuan, *A Review on Recent Development of Cooling Technologies for Concentrated Photovoltaics (CPV) Systems*. Energies, 2018. **11**(12): p. 3416.
5. Lei, S., Y. Shi, and G. Chen, *A lithium-ion battery-thermal-management design based on phase-change-material thermal storage and spray cooling*. Applied Thermal Engineering, 2020. **168**: p. 114792.
6. Xu, R., G. Wang, and P. Jiang, *Spray Cooling on Enhanced Surfaces: A Review of the Progress and Mechanisms*. Journal of Electronic Packaging, 2021. **144**(1).
7. Qiao, Y.M. and S. Chandra, *Spray Cooling Enhancement by Addition of a Surfactant*. Journal of Heat Transfer, 1998. **120**(1): p. 92-98.
8. Liang, G. and I. Mudawar, *Review of spray cooling – Part 1: Single-phase and nucleate boiling regimes, and critical heat flux*. International Journal of Heat and Mass Transfer, 2017. **115**: p. 1174-1205.
9. Visaria, M. and I. Mudawar, *Theoretical and experimental study of the effects of spray inclination on two-phase spray cooling and critical heat flux*. International Journal of Heat and Mass Transfer, 2008. **51**(9): p. 2398-2410.
10. Chen, C., S. Li, X. Wu, Y. Wang, and F. Kang, *Analysis of droplet size uniformity and selection of spray parameters based on the biological optimum particle size theory*. Environmental Research, 2022. **204**: p. 112076.
11. Cebo-Rudnicka, A., Z. Malinowski, and A. Buczek, *The influence of selected parameters of spray cooling and thermal conductivity on heat transfer coefficient*. International Journal of Thermal Sciences, 2016. **110**: p. 52-64.
12. Horacek, B., K.T. Kiger, and J. Kim, *Single nozzle spray cooling heat transfer mechanisms*. International Journal of Heat and Mass Transfer, 2005. **48**(8): p. 1425-1438.
13. Zhu, X., W. Yang, Y. Yao, Y. Geng, and J. Zhou, *Spray and vaporization enhancement of liquid fuel with the assist of porous media and heating*. Applied Thermal Engineering, 2023. **226**: p. 120329.
14. Tsutsumi, K., J. Kubota, A. Hosokawa, S. Ueoka, H. Nakano, A. Kuramoto, and I. Sumi, *Effect of Spray Thickness and Collision Pressure on Spray Cooling Capacity in a Continuous Casting Process*. steel research international, 2018. **89**(7): p. 1700567.
15. Tian, J.-M., B. Chen, D. Li, and Z.-F. Zhou, *Transient spray cooling: Similarity of dynamic heat flux for different cryogen, nozzles and substrates*. International Journal of Heat and Mass Transfer, 2017. **108**: p. 561-571.
16. Bao, M., F. Wang, Y. Guo, L. Gong, and S. Shen, *Experimental study of two-phase heat transfer of droplet impact on liquid film*. Physics of Fluids, 2022. **34**(4).
17. Ruan, Y., Y. Hou, R. Xue, G. Luo, K. Zhu, X. Liu, and L. Chen, *Effects of operational parameters on liquid nitrogen spray cooling*. Applied Thermal Engineering, 2019. **146**: p. 85-91.
18. Yeganehdoust, F., R. Attarzadeh, I. Karimfazli, and A. Dolatabadi, *A numerical analysis of air entrapment during droplet impact on an immiscible liquid film*. International Journal of Multiphase Flow, 2020. **124**: p. 103175.
19. Lee, S.H., N. Hur, and S. Kang, *A numerical analysis of drop impact on liquid film by using a level set method*. Journal of Mechanical Science and Technology, 2011. **25**(10): p. 2567-2572.
20. Guo, Y., L. Wei, G. Liang, and S. Shen, *Simulation of droplet impact on liquid film with CLSVOF*. International Communications in Heat and Mass Transfer, 2014. **53**: p. 26-33.

21. Shen, M. and B.Q. Li, *Phase Field Modeling of Air Entrapment in Binary Droplet Impact with Solidification Microstructure Formation*. Coatings, 2022. **12**(12): p. 1990.
22. Xie, Z., G.F. Hewitt, D. Pavlidis, P. Salinas, C.C. Pain, and O.K. Matar, *Numerical study of three-dimensional droplet impact on a flowing liquid film in annular two-phase flow*. Chemical Engineering Science, 2017. **166**: p. 303-312.
23. Tao, J., D. Chen, Z. Lin, and Z. Zhu, *Numerical simulation analysis of symmetric impact of two droplets on a liquid film*. Physics of Fluids, 2022. **34**(9).
24. Cao, Y., J. Wang, and C. Zhu, *Numerical Simulation of Microscale Oblique Droplet Impact on Liquid Film*. Aerospace, 2023. **10**(2): p. 119.
25. Trujillo, M.F., J. Alvarado, E. Gehring, and G.S. Soriano, *Numerical Simulations and Experimental Characterization of Heat Transfer From a Periodic Impingement of Droplets*. Journal of Heat Transfer, 2011. **133**(12).
26. Liang, G., L. Chen, Y. Chen, and S. Shen, *Interfacial phenomena and heat transfer associated with multi-droplet impact on flowing liquid film*. Numerical Heat Transfer, Part A: Applications, 2020. **77**(1): p. 80-89.
27. Li, D. and X. Duan, *Numerical analysis of droplet impact and heat transfer on an inclined wet surface*. International Journal of Heat and Mass Transfer, 2019. **128**: p. 459-468.
28. Osher, S. and J.A. Sethian, *Fronts propagating with curvature-dependent speed: Algorithms based on Hamilton-Jacobi formulations*. Journal of computational physics, 1988. **79**(1): p. 12-49.
29. Lee, W.H., *Pressure iteration scheme for two-phase flow modeling*. Multiphase Transport Fundamentals, Reactor Safety, Applications, 1980: p. 407-432.